Acta Crystallographica Section C
Crystal Structure Communications
ISSN 0108-2701

Cocrystals of 2,3,5,6-tetrafluorobenzene-1,4-diol with diaza aromatic compounds

Agnieszka Czapik and Maria Gdaniec*

Faculty of Chemistry, Adam Mickiewicz University, 60-780 Poznań, Poland
Correspondence e-mail: magdan@amu.edu.pl

Received 27 May 2010
Accepted 7 June 2010
Online 11 June 2010

2,3,5,6-Tetrafluorobenzene-1,4-diol easily forms cocrystals with heteroaromatic bases containing the pyrazine unit. In the 1:1 complexes with pyrazine, $C_6H_2F_4O_2\cdot C_4H_4N_2$, (I), and quinoxaline, $C_6H_2F_4O_2\cdot C_8H_6N_2$, (II), the crystal components are linked *via* O—H···N hydrogen bonds into one-dimensional chains. With the largest base, phenazine, the 1:2 benzenediol–phenazine complex, $C_6H_2F_4O_2\cdot 2C_{12}H_8N_2$, (III), was obtained, with the molecules linked *via* O—H···N interactions into a discrete heterotrimer. In all three cocrystals, the two types of molecules are organized into layers *via* softer C—H···O and C—H···F interactions and π–π stacking interactions, with stronger hydrogen bonds linking molecules of adjacent layers. In (II) and (III), molecules are arranged into heterostacks, whereas in (I) separate stacks are formed by the heterocyclic base and the benzenediol molecule.

Comment

Among the intermolecular interactions used to guide supramolecular synthesis are conventional (hard) hydrogen bonds, weak (soft) hydrogen bonds, halogen bonds, aromatic-ring interactions and electrostatic interactions. Very early on, strong hydrogen bonds were recognized as a powerful organizing force determining the structure of many molecular crystals. However, the formation of any supramolecular structure is the result of a large number of interactions, and the much weaker forces, often numerous and acting cooperatively, can play a decisive role in determinining the overall structure and stability of a supramolecular assembly.

The diaza aromatic weak bases phenazine (PHZ), quinoxaline (QX) and pyrazine (PYZ) have a similar potential to form molecular complexes through hard hydrogen bonds. However, the recognition process, which also involves weaker interactions with the aromatic π system and the C—H groups, can proceed differently, influencing the stoichiometry and the packing mode of the substrates in the crystal structures. These three aromatic heterocycles are considered as good supramolecular substrates. For example, Thalladi *et al.* (2000) have shown that PHZ cocrystallizes with hydroquinone (HQ) in a 2:1 molar ratio to form a square-grid type host network constructed from stacks of PHZ with the diphenol guest molecules accommodated in channels, where they interact with PHZ *via* hard hydrogen bonds, weak hydrogen bonds and edge-to-face aromatic interactions. Some other diphenols give a similar packing arrangement and their stoichiometries also do not conform with the simple considerations of hydrogen-bond requirements (Thalladi *et al.*, 2000). Reducing the size of the aromatic-ring system and lowering the symmetry of the hetorocyclic base has basically no influence on the overall packing mode, as shown by the structure of QX–HQ (2/1) (Kadzewski & Gdaniec, 2006).

Cocrystals of the three above-mentioned diaza heterocycles with 3,6-dihydroxy-1,4-benzoquinones have been extensively studied in relation to the interesting ferroelectric properties exhibited by some members of this new group of materials (Horiuchi, Ishii *et al.*, 2005; Horiuchi, Kumai & Tokura, 2005; Gotoh, Asaji & Ishida, 2007). They generally differ both in the stoichiometry and in the packing mode observed in the cocrystals compared with those with HQ. 2,5-Dibromo-3,6-dihydroxy-1,4-benzoquinone (bromanilic acid, BrA; Tomura & Yamashita, 2000) and 2,5-chloro-3,6-dihydroxy-1,4-benzoquinone (chloranilic acid, ClA; Gotoh, Asaji & Ishida, 2007; Gotoh, Nagoshi & Ishida, 2007) cocrystallize with PHZ or QX in a 1:1 ratio and the component molecules are connected alternately by O—H···N hydrogen bonds into robust polymeric chains. In addition, the aromatic heterobases and diacids are arranged into segregated stacks *via* offset face-to-face π–π stacking interactions. In the case of the cocrystal PYZ–ClA (2/1), partial proton transfer from ClA to the base influences the stoichiometry of the complex (Gotoh *et al.*, 2008).

2,3,5,6-Tetrafluorobenzene-1,4-diol (TFHQ) has a similar hydrogen-bond potential to HQ, but the electron density of the aromatic ring is substantially reduced due to the presence of the four electron-withdrawing F substituents. This has to have an impact on the ability of the TFHQ aromatic ring to participate in the edge-to-face interactions that are of primary importance in the formation of channel-type structures in cocrystals of HQ with PHZ or QX (Thalladi *et al.*, 2000; Kadzewski & Gdaniec, 2006). On the other hand, the lowered electron density of the benzene ring in TFHQ should promote the formation of mixed π stacks by interaction of TFHQ with aromatic heterobases, by analogy with the robust packing motif found in the arene–perfluoroarene systems (Collings *et al.*, 2002, and references therein). To see how the substitution of hydroquinone C—H groups by C—F groups affects the intermolecular interactions and crystal packing modes in two-component systems composed of a diaza aromatic base and hydroquinone, three cocrystals, namely TFHQ–PYZ (1/1), (I), TFHQ–QX (1/1), (II), and TFQX–PHZ (1/2), (III), were obtained and their structures studied by X-ray analyses.

The molecular structures of cocrystals (I)–(III), together with their atom-numbering schemes, are shown in Fig. 1. TFHQ cocrystallizes with PYZ and QX in a 1:1 molar ratio, as

  doi:10.1107/S0108270110021736

could be predicted from the number of hydrogen-bond donor and acceptor groups. The cocrystal of PHZ and TFHQ contains the two components in a 2:1 ratio, *i.e.* the stoichiometry is the same as in the cocrystal of PHZ and HQ (Thalladi *et al.*, 2000). In (I), both crystal components lie on inversion

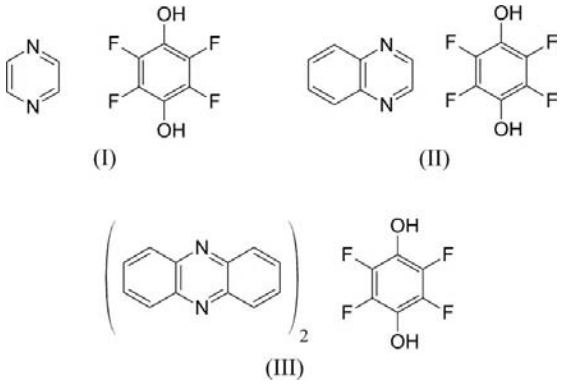

centres. In (III), only the TFHQ molecule is located on a special position of C_i symmetry, whereas in (II), all the molecules are in general positions. The geometry of TFHQ in the three cocrystals is virtually the same (Tables 1, 3 and 5), with the C—O bond lengths ranging from 1.3504 (15) to 1.352 (3) Å, and the endocyclic angles at the C atoms attached to the OH groups in the range 115.6 (2)–115.76 (12)°. A value smaller than 120° for this bond angle is consistent with the electron-donating character of the hydroxy groups (Domenicano *et al.*, 1975). Nevertheless, the observed values are *ca* 1.5° smaller than in the TFHQ molecule in its anhydrous and hydrated forms (117.1–117.5°; Thalladi *et al.*, 1999; Rusak & Gdaniec, 2006). Significant differences are also found in the C—O bond lengths, which in the above-mentioned crystalline forms of TFHQ are longer (1.362–1.367 Å). All these changes in the molecular geometry can be attributed to hydrogen-bond interactions involving the hydroxy group. In cocrystals (I)–(III), the OH groups donate an H atom to the O—H···N hydrogen bond formed with the weak organic bases and the geometry of these hydrogen bonds, with O···N distances in the range 2.7257 (14)–2.791 (3) Å (Tables 2, 4 and 6), points to a strong interaction. This should increase significantly the electron density at the phenolic donor group, resulting in the observed geometric changes in the molecular structure of TFHQ. The O—H···N hydrogen bonds observed in the three cocrystals with TFHQ are also shorter than the hydrogen bonds formed by HQ with PHZ (2.815 Å; Thalladi *et al.*, 2000) and by HQ with QX [2.8425 (18) Å; Kadzewski & Gdaniec, 2006], in accord with the increased acidity of TFHQ relative to HQ.

The hydrogen-bonding O—H···N interaction between the two cocrystal components is the strongest specific interaction that organizes the molecules into polymeric chains [(I) and (II)] or into discrete heterotrimers [(III)]. To avoid repulsive H···F interactions between molecules brought close together by hydrogen bonding, they have to twist substantially along the O···N line of the intermolecular O—H···N hydrogen bond. The dihedral angle between interacting molecules increases slightly with the increase of the aromatic system of the base and ranges from 43.97 (7)° in (I) through 48.50 (4) and 47.63 (4)° in (II) to 49.32 (2)° in (III), whereas the shortest H···F distance between the hydrogen-bonded components changes from 2.62 Å in (II) to 2.81 Å in (III). Similar twist angles were observed in the cocrystals of BrA with QX (49.8°) and PHZ (45.3°), leading to H···O distances between hydrogen-bonded partners of 2.80 and 2.57 Å, respectively (Tomura & Yamashita, 2000).

The crystal packing in (I), together with the most important intermolecular synthons, is illustrated in Fig. 2. Alternating PYZ and TFHQ molecules, connected *via* O—H···N hydrogen bonds (Table 2), form polymeric chains extending along [$\bar{1}$11]. Another chain is formed in the [1$\bar{1}$1] direction *via* softer C—H···O and C—H···F interactions. The latter corrugated chains stack one above the other in a manner

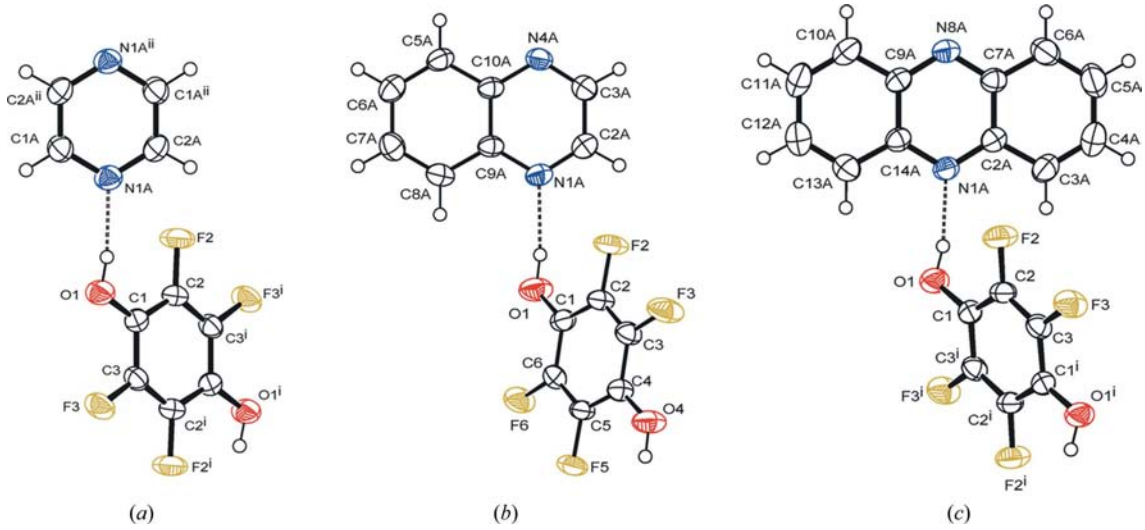

Figure 1
The molecular structures of (*a*) (I), (*b*) (II) and (*c*) (III), showing the atom-numbering schemes. Displacement ellipsoids are drawn at the 50% probability level and H atoms are shown as small spheres of arbitrary radii. Hydrogen bonds are shown as dashed lines. [Symmetry codes: (i) $1-x, 1-y, 1-z$: (ii) $2-x, -y, -z$.]

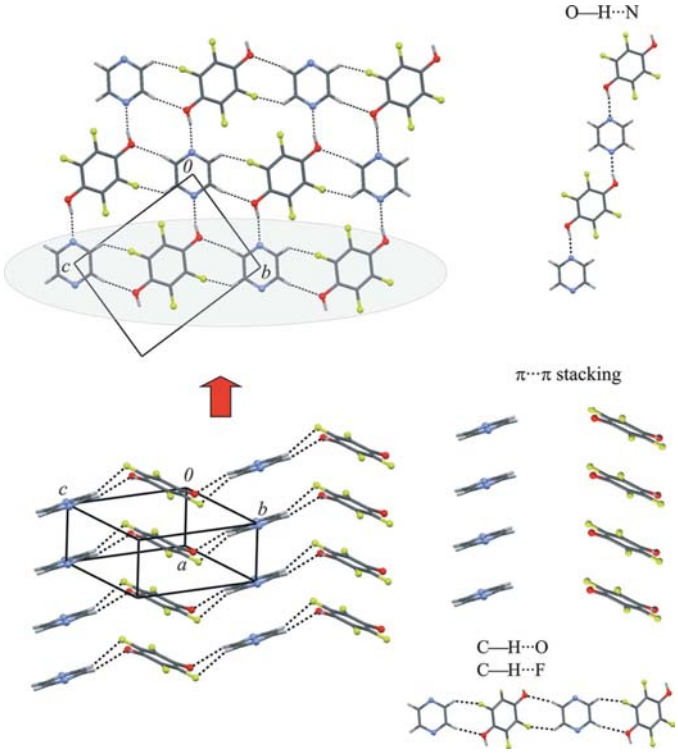

Figure 2
The crystal packing of (I), showing the intermolecular synthons. O, F and N atoms are represented as spheres of arbitrary radii. Hydrogen bonds are shown as dashed lines.

leading to the formation of separate stacks of PZ and TFHQ *via* offset face-to-face π–π stacking interactions. In effect, the softer interactions assemble the molecules into (011) layers, whereas the hard O—H···N interactions connect molecules from adjacent layers.

As illustrated in Fig. 3, the polymeric chains formed *via* O—H···N hydrogen bonds in (II) differ in shape from those in (I), as the two chains have different rod group symmetries. Whereas the chains in (I) are centrosymmetric and belong to the $P\overline{1}$ rod group, in (II) the hydrogen-bonded chains exhibit a noncrystallographic centrosymmetric structure belonging to the $P12_1/m1$ rod group, with the twofold screw axis directed along the *c* axis; the pseudo-mirror plane is perpendicular to the QX aromatic system and the pseudo-inversion centre is at the centroid of the TFHQ benzene ring. The structure and symmetry of this chain resemble very closely those of the hydrogen-bonded chain of the QNX–BrA (1/1) cocrystal (Tomura & Yamashita, 2000). Nevertheless, the packing modes of these centrosymmetric assemblies are different, because in (II) the crystal structure is chiral, as shown by the $P2_12_12_1$ space-group symmetry. Unlike in cocrystals of QX with HQ, ClA or BrA, π–π stacking interactions between QX and TFHQ result in heterostacks that are formed along the *b* axis, with alternating aromatic bases and benzenediol molecules. Within the stack, the distances between the centroid of TFHQ and the centroids of the pyrazine (symmetry code: $1-x, \frac{1}{2}+y, \frac{3}{2}-z$) and benzene (symmetry code: $1-x, -\frac{1}{2}+y, \frac{3}{2}-z$) rings of QX are 3.824 (2) and 3.640 (2) Å, respectively. Molecules from neighbouring stacks are connected into (001)

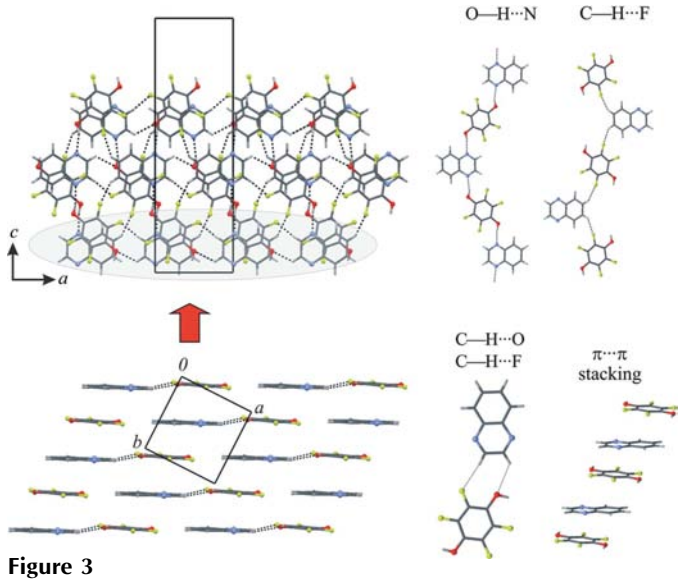

Figure 3
The crystal packing of (II), showing the intermolecular synthons. O, F and N atoms are represented as spheres of arbitrary radii. Hydrogen bonds are shown as dashed lines.

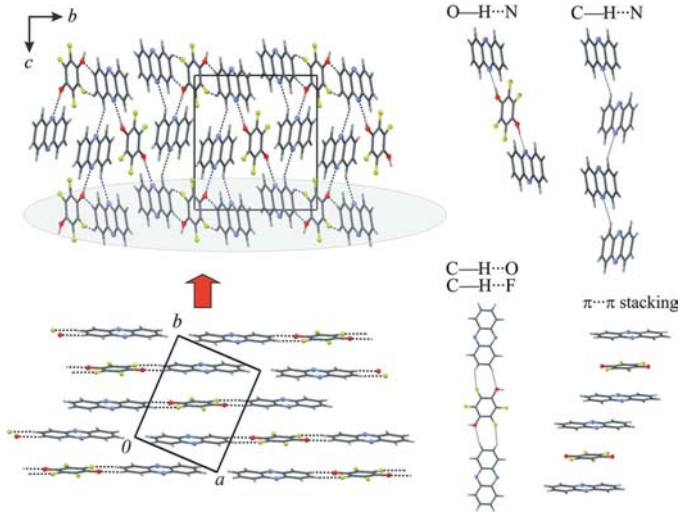

Figure 4
The crystal packing of (III), showing the intermolecular synthons. O, F and N atoms are represented as spheres of arbitrary radii. Hydrogen bonds are shown as dashed lines.

layers by soft C—H···O and C—H···F interactions to form heterodimers. Again, the molecules are arranged *via* soft interactions into layer-type assemblies, whereas the strongest O—H···N interactions operate between molecules from adjacent layers. In addition to the O—H···N hydrogen bonds, molecules from adjacent layers are also connected *via* C—H···F interactions (Table 4).

Despite the change in stoichiometry, layers formed *via* softer C—H···O and C—H···F hydrogen bonds and offset face-to-face stacking interactions are also found in (III). The molecules are connected *via* soft C—H···O and C—H···F hydrogen bonds into heterotrimers that stack into (001) layers *via* π–π interactions (Fig. 4, lower left; Table 6). The heterostacks thus formed are extended along the *b* axis and each TFHQ molecule is surrounded by two PHZ molecules, with a

distance between the TFHQ centroid and the centroid of the PHZ pyrazine unit of 3.7053 (7) Å. In turn, each PHZ molecule in the stack is surrounded by TFHQ and PHZ molecules, and the distance between the centroids of the benzene and pyrazine fragments (symmetry code: $-x, 1-y, -z$) of the two PHZ molecules is 3.6059 (8) Å. As in the cocrystals (I) and (II), hard O—H···N hydrogen bonds link molecules from adjacent layers (Fig. 4, upper left), but only discrete heterotrimers are formed. There is also a weak interlayer C—H···N interaction involving PHZ molecules.

In summary, layer-type assemblies generated by weak hydrogen bonds and π–π stacking interactions, with stronger hydrogen bonds acting between the layers, are a common structural feature of the cocrystals formed by the benzenediols HQ or TFHQ with the diaza aromatic heterobases QX or PHZ. In cocrystals with HQ, the layer-type assemblies are similarly constructed, with face-to-face stacking interactions arranging the heterocyclic molecules into homostacks, and HQ molecules, involved in edge-to-face interactions with the heterobase and in weak hydrogen bonds, inserted between the stacks. In turn, TFHQ molecules, with reduced electron density of the aromatic π system and increased electron density of the lateral groups, prefer to form heterostacks and weak hydrogen bonds with the heterobase. Nevertheless, the layer-type assemblies composed from the aromatic heterocycles and TFHQ involved in a similar 'set' of intermolecular interactions have a different structure in the case of cocrystals with QX and PHZ.

Experimental

Cocrystals (I)–(III) were obtained by dissolving 2,3,5,6-tetrafluorobenzene-1,4-diol and the corresponding aromatic diaza heterocycles (Aldrich) in a 1:1 molar ratio in cold [for (I) and (II)] or hot [for (III)] ethanol. The solutions were allowed to evaporate slowly and the precipitated crystals, suitable for X-ray analysis, were separated by filtration.

Compound (I)

Crystal data

$C_6H_2F_4O_2\cdot C_4H_4N_2$
M_r = 262.17
Triclinic, $P\overline{1}$
a = 3.6671 (10) Å
b = 7.585 (2) Å
c = 9.582 (2) Å
α = 88.14 (2)°
β = 85.67 (2)°
γ = 77.41 (2)°
V = 259.34 (11) Å^3
Z = 1
Mo $K\alpha$ radiation
μ = 0.17 mm^{-1}
T = 294 K
0.60 × 0.15 × 0.05 mm

Data collection

Kuma KM-4 CCD diffractometer in κ geometry
1921 measured reflections
917 independent reflections
791 reflections with $I > 2\sigma(I)$
R_{int} = 0.041

Refinement

$R[F^2 > 2\sigma(F^2)]$ = 0.048
$wR(F^2)$ = 0.132
S = 1.08
917 reflections
82 parameters
H-atom parameters constrained
$\Delta\rho_{max}$ = 0.37 e Å^{-3}
$\Delta\rho_{min}$ = −0.31 e Å^{-3}

Table 1
Selected geometric parameters (Å, °) for (I).

O1—C1	1.352 (2)		
O1—C1—C2	125.50 (15)	C2—C1—C3	115.62 (15)
O1—C1—C3	118.87 (14)		

Table 2
Hydrogen-bond geometry (Å, °) for (I).

D—H···A	D—H	H···A	D···A	D—H···A
O1—H1O···N1A	0.85	1.90	2.7343 (19)	167
C2A—H2A···F3^{i}	0.96	2.64	3.350 (2)	131
C3A—H3A···O1^{ii}	0.96	2.62	3.538 (2)	159

Symmetry codes: (i) $x+1, y-1, z$; (ii) $-x+1, -y+1, -z$.

Compound (II)

Crystal data

$C_6H_2F_4O_2\cdot C_8H_6N_2$
M_r = 312.22
Orthorhombic, $P2_12_12_1$
a = 7.2094 (5) Å
b = 7.4290 (4) Å
c = 23.585 (13) Å
V = 1263.2 (7) Å^3
Z = 4
Mo $K\alpha$ radiation
μ = 0.15 mm^{-1}
T = 294 K
0.60 × 0.40 × 0.40 mm

Data collection

Kuma KM-4 CCD diffractometer in κ geometry
6629 measured reflections
1324 independent reflections
1208 reflections with $I > 2\sigma(I)$
R_{int} = 0.037

Table 3
Selected geometric parameters (Å, °) for (II).

O1—C1	1.352 (3)	O4—C4	1.355 (3)
O1—C1—C2	124.73 (19)	O4—C4—C5	124.83 (18)
O1—C1—C6	119.7 (2)	O4—C4—C3	119.6 (2)
C2—C1—C6	115.6 (2)	C5—C4—C3	115.5 (2)

Table 4
Hydrogen-bond geometry (Å, °) for (II).

D—H···A	D—H	H···A	D···A	D—H···A
O1—H1O···N1A	0.85	1.94	2.776 (3)	168
O4—H4O···N4A^{i}	0.85	1.98	2.791 (3)	160
C2A—H2A···F3^{ii}	0.96	2.45	3.399 (3)	169
C3A—H3A···O4^{ii}	0.96	2.61	3.282 (3)	127
C7A—H7A···F2^{iii}	0.96	2.53	3.156 (3)	123
C6A—H6A···F5^{iv}	0.96	2.54	3.068 (3)	114

Symmetry codes: (i) $-x+\frac{3}{2}, -y+1, z+\frac{1}{2}$; (ii) $-x+2, y-\frac{1}{2}, -z+\frac{3}{2}$; (iii) $x-1, y, z$; (iv) $-x+\frac{1}{2}, -y+1, z-\frac{1}{2}$.

Table 5
Selected geometric parameters (Å, °) for (III).

O1—C1	1.3504 (15)		
O1—C1—C2	125.05 (12)	C2—C1—C3^{i}	115.76 (12)
O1—C1—C3^{i}	119.19 (11)		

Symmetry code: (i) $-x+1, -y+1, -z+1$.

Table 6
Hydrogen-bond geometry (Å, °) for (III).

D—H···A	D—H	H···A	D···A	D—H···A
O1—H1O···N1A	0.85	1.89	2.7257 (14)	166
C3A—H3···N8A^{ii}	0.96	2.60	3.4958 (18)	155
C5A—H5···O1^{iii}	0.96	2.48	3.4203 (18)	165
C4A—H4···F3^{iv}	0.96	2.53	3.3445 (17)	143

Symmetry codes: (ii) $x+\frac{1}{2}, -y+\frac{1}{2}, z+\frac{1}{2}$; (iii) $x+\frac{1}{2}, -y+\frac{1}{2}, z-\frac{1}{2}$; (iv) $-x+\frac{3}{2}, y-\frac{1}{2}, -z+\frac{1}{2}$.

Refinement

$R[F^2 > 2\sigma(F^2)] = 0.031$
$wR(F^2) = 0.084$
$S = 1.06$
1324 reflections
200 parameters
H-atom parameters constrained
$\Delta\rho_{max} = 0.17$ e Å^{-3}
$\Delta\rho_{min} = -0.15$ e Å^{-3}

Compound (III)

Crystal data

$C_6H_2F_4O_2\cdot 2C_{12}H_8N_2$
$M_r = 542.48$
Monoclinic, $P2_1/n$
$a = 9.1482$ (5) Å
$b = 11.0393$ (6) Å
$c = 12.4185$ (8) Å
$\beta = 102.585$ (5)°
$V = 1224.01$ (12) Å^3
$Z = 2$
Mo $K\alpha$ radiation
$\mu = 0.12$ mm^{-1}
$T = 294$ K
0.40 × 0.40 × 0.30 mm

Data collection

Kuma KM-4 CCD diffractometer in κ geometry
8327 measured reflections
2476 independent reflections
1862 reflections with $I > 2\sigma(I)$
$R_{int} = 0.024$

Refinement

$R[F^2 > 2\sigma(F^2)] = 0.041$
$wR(F^2) = 0.125$
$S = 1.07$
2476 reflections
182 parameters
H-atom parameters constrained
$\Delta\rho_{max} = 0.23$ e Å^{-3}
$\Delta\rho_{min} = -0.20$ e Å^{-3}

In (II), in the absence of significant anomalous scattering effects, Friedel pairs were averaged. The H atoms from the O—H groups were located in electron-density difference maps. In the final cycles of refinement, they and the C-bound H atoms were included in calculated postions and treated as riding atoms, with O—H = 0.85 Å and C—H = 0.96 Å, and with U_{iso}(H) = 1.2U_{eq}(O,C).

For all compounds, data collection: *CrysAlis CCD* (Oxford Diffraction, 2004); cell refinement: *CrysAlis CCD*; data reduction: *CrysAlis RED* (Oxford Diffraction, 2004); program(s) used to solve structure: *SHELXS97* (Sheldrick, 2008); program(s) used to refine structure: *SHELXL97* (Sheldrick, 2008); molecular graphics: *ORTEP-3 for Windows* (Farrugia, 1997) and *Mercury* (Macrae *et al.*, 2006); software used to prepare material for publication: *SHELXL97*.

The authors thank Mr Paweł Rusak for assistance at the start of this project.

Supplementary data for this paper are available from the IUCr electronic archives (Reference: SU3047). Services for accessing these data are described at the back of the journal.

References

Collings, J. C., Roscoe, K. P., Robins, E. G., Batsanov, A. S., Stimson, L. M., Howard, J. A. K., Clark, S. J. & Marder, T. B. (2002). *New J. Chem.* **26**, 1740–1746.
Domenicano, A., Vaciago, A. & Coulson, C. A. (1975). *Acta Cryst.* B**31**, 221–234.
Farrugia, L. J. (1997). *J. Appl. Cryst.* **30**, 565.
Gotoh, K., Asaji, T. & Ishida, H. (2007). *Acta Cryst.* C**63**, o17–o20.
Gotoh, K., Asaji, T. & Ishida, H. (2008). *Acta Cryst.* C**64**, o550–o553.
Gotoh, K., Nagoshi, H. & Ishida, H. (2007). *Acta Cryst.* E**63**, o4295.
Horiuchi, S., Ishii, F., Kumai, R., Okimoto, Y., Tachibana, H., Nagaosa, N. & Tokura, Y. (2005). *Nat. Mater.* **4**, 163–166.
Horiuchi, S. F., Kumai, R. & Tokura, Y. (2005). *J. Am. Chem. Soc.* **127**, 5010–5011.
Kadzewski, A. & Gdaniec, M. (2006). *Acta Cryst.* E**62**, o3498–o3500.
Macrae, C. F., Edgington, P. R., McCabe, P., Pidcock, E., Shields, G. P., Taylor, R., Towler, M. & van de Streek, J. (2006). *J. Appl. Cryst.* **39**, 453–457.
Oxford Diffraction (2004). *CrysAlis CCD* and *CrysAlis RED*. Versions 1.171. Oxford Diffraction Ltd, Abingdon, Oxfordshire, England.
Rusak, P. & Gdaniec, M. (2006). *Acta Cryst.* E**62**, o1650–o1651.
Sheldrick, G. M. (2008). *Acta Cryst.* A**64**, 112–122.
Thalladi, V. R., Smolka, T., Boese, R. & Sustmann, R. (2000). *CrystEngComm*, **2**, 96–101.
Thalladi, V. R., Weiss, H.-C., Boese, R., Nangia, A. & Desiraju, G. R. (1999). *Acta Cryst.* B**55**, 1005–1013.
Tomura, M. & Yamashita, Y. (2000). *CrystEngComm*, **2**, 92–95.